**THE EUROPEAN
PHYSICAL JOURNAL
SPECIAL TOPICS**

Regular Article

Electroformation of giant unilamellar vesicles from large liposomes

Huriye D. Uzun[1,2], Zeynep Tiris[1], Maiko Czarnetzki[1], Rosa L. López-Marqués[2],
and Thomas Günther Pomorski[1,2,a]

[1] Department of Molecular Biochemistry, Faculty of Chemistry and Biochemistry, Ruhr University Bochum, 44780 Bochum, Germany
[2] Department of Plant and Environmental Sciences, University of Copenhagen, 1871 Frederiksberg C, Denmark

Abstract Giant unilamellar vesicles (GUVs) are widely used as model systems for biological membranes to study membrane-related processes in a precisely controlled in vitro environment, owing to their biophysical properties. The classical technique for the formation of giant liposomes starts with the dissolution of lipids or lipid mixtures in an organic solvent, which is then deposited as a thin lipid solution film on a support substrate. In this study, we present a comprehensive analysis investigating the effect of different lipid compositions on the generation of GUVs from preformed liposomes under non-ionic and ionic conditions. For all liposome types tested, the electroformation process, whether performed on indium tin oxide-coated glass slides or platinum wires, consistently produced GUVs that typically ranged in size from 5 to 20 µm. However, the yield of GUVs varied depending on the specific non-ionic or ionic conditions and the lipid composition of the preformed liposomes used. In general, the resulting population of giant vesicles was predominantly characterised by the presence of unilamellar and multivesicular vesicles. These findings have the potential to improve the refinement of protocol parameters for the formation of GUVs containing membrane proteins and for the study of the effects of lipid composition on membrane protein activity.

1 Introduction

Giant unilamellar vesicles (GUVs) are a fundamental tool in the fields of membrane biophysics and cellular biology, serving as artificial vesicles that mimic cell membranes [1]. Their size, ranging from 1 to 100 µm, allows them to closely resemble eukaryotic cells, making them ideal candidates for studying cellular processes in a controlled environment by optical microscopic techniques. GUVs offer the unique advantage of precise control over their molecular composition and environmental conditions and are well suited for micromanipulation experiments and mechanical measurements by micropipette aspiration or flickering spectroscopy [2]. This makes them invaluable model systems for studying various aspects of lipid membranes, including membrane thermodynamics [3], curvature [4], membrane domains [5, 6], membrane fusion [5], lateral structure [7], bending stiffness [8], and lipid–protein interactions [9]. As a closed compartment, GUVs also facilitate the analysis of membrane protein activity in a native-like environment upon their reconstitution [10]. In contrast to bulk assays, which provide averaged values, GUVs allow for the individualised measurement of parameters such as morphology, size and amount of protein. This fine level of detail greatly improves the accuracy of experimental results and facilitates a deeper understanding of cellular processes and interactions. Furthermore, GUVs are useful for applications in bottom-up synthetic biology and biomedicine [11–13].

An extensively employed method for generating GUVs is based on electroformation [14]. This technique involves dissolving lipids or lipid mixtures in organic solvents. The resulting lipid solution is then spread as a thin film on specialised surfaces, such as indium tin oxide (ITO)-coated glass or platinum wires [14, 15]. After solvent removal, the liposomes are hydrated in the presence of an aqueous buffer and an alternating current (AC) field. Electro-osmotic and dielectric forces are proposed to play an essential role in the swelling of the lipid film, leading to the

---

[a] e-mail: Thomas.Guenther-Pomorski@ruhr-uni-bochum.de (corresponding author)

Table 1 Compositions of buffers used in this study

Buffers	Compositions
Lipid buffer	50 mM K_2SO_4, 10 mM MOPS-KOH, pH 7
Non-ionic GUV formation buffer	299 mM sucrose, 1 mM MOPS-KOH, pH 7
Ionic K_2SO_4 GUV formation buffer	50 mM K_2SO_4, 140 mM sucrose, 10 mM MOPS-KOH, pH 7
Ionic KCl GUV formation buffer	100 mM KCl, 190 mM sucrose, 10 mM MOPS-KOH, pH 7
Ionic NaCl GUV formation buffer	100 mM NaCl, 190 mM sucrose, 10 mM MOPS-KOH, pH 7
Non-ionic microscopy buffer	299 mM glucose, 1 mM MOPS-KOH, pH 7
Ionic K_2SO_4 microscopy buffer	50 mM K_2SO_4, 140 mM glucose, 10 mM MOPS-KOH, pH 7
Ionic KCl microscopy buffer	100 mM KCl, 190 mM glucose, 10 mM MOPS-KOH, pH 7
Ionic NaCl microscopy buffer	100 mM NaCl, 190 mM glucose, 10 mM MOPS-KOH, pH 7

formation of giant vesicles [16, 17]. A number of excellent studies have revealed the optimal conditions for the preparation of protein-free GUVs from thin lipid films under non-ionic and ionic conditions [18–20].

Electroformation has also been used for the preparation of GUVs containing membrane proteins. In this case, the strategy is based on two-step procedures utilising first preformed large unilamellar proteoliposomes as starting material for the generation of protein-containing GUVs. The advantage of this two-step approach is that the protein functionality in the proteoliposomes can be tested before the GUVs are prepared [21–23]. In addition, proteoliposomes can be customised in a variety of ways by fine-tuning the lipid composition [24]. Lipids that promote protein stability and/or control protein function can be used, and modified lipids, such as pH sensors or fluorophores, can be incorporated. The approach has been applied successfully to several structurally and functionally unrelated membrane proteins, including an ER membrane extract containing constitutively active phospholipid scramblases [25], the sarcoplasmic reticulum Ca^{2+}-ATPase [26], Na^+/K^+ ATPase [27, 28], the H^+ transporter bacteriorhodopsin [26, 29], hamster P-glycoprotein [21], OppA translocator [22, 23], a voltage-gated K^+ channel [30], a voltage-dependent anion-selective channel [31], integrins [32], SNARE proteins [33, 34] and an aquaporin [35]. The diversity of the membrane proteins reconstituted into GUVs demonstrates the versatility of this system (SI Table S1).

Here, we conducted a comprehensive investigation of the influence of different phospholipid compositions, including different unsaturated, as well as charged and uncharged phospholipids, in the preparation of GUVs from preformed liposomes. We employed both non-ionic and ionic aqueous buffers during the rehydration process and made adjustments to the AC field in the presence of ions. The primary objective of our study was to examine the effects of lipid properties (saturation and charge), ions, and their concentrations during rehydration on the quality of GUVs. The findings from this study will contribute to optimising the protocol parameters for GUV electroformation using proteoliposomes and provide valuable insights for future research involving membrane protein reconstitution.

2 Experimental section

2.1 Materials

Phospholipids 1-palmitoyl-2-oleoyl-phosphatidylcholine (POPC), 1,2-dioleoyl-phosphatidylcholine (DOPC), -phosphatidylglycerol (DOPG), -phosphatidylethanolamine (DOPE), -phosphatidylserine (DOPS), and N-[1-(2,3-dioleyl)propyl]-N,N,N-trimethylammonium chloride (DOTAP) were purchased from Avanti Polar Lipids Inc. (Alabaster, AL, USA), and 1,2-dioleoyl-*sn*-glycero-3-phosphoethanolamine headgroup labelled with ATTO 488 (ATTO488-DOPE) was obtained from ATTO-TEC GmbH (Siegen, Germany). All other chemicals and reagents were from Sigma-Aldrich (München, Germany), if not stated otherwise. All solutions used for vesicles were filter-sterilised through a polyethersulfone membrane with a pore size of 0.2 µm (Filtropur, Sarstedt AG & Co. KG, Nümbrecht, Germany). The composition of the buffers used is given in Table 1.

2.2 Liposome preparation

Large liposomes were prepared by gentle hydration of lipid films. Briefly, lipids in chloroform were transferred into glass tubes. For the binary lipid mixtures, DOPC was mixed with the indicated phospholipid at a molar ratio of 7:3. In addition, 0.1/0.2 mol% ATTO488-DOPE were added to the bulk lipids. The solvent was removed overnight at 250 mbar by rotary evaporation. The lipid film (5 mg) was rehydrated in 1 mL lipid buffer or 1 mL chloroform

by vortexing in the presence of a glass bead (5 mm diameter) for 10 min, yielding a final lipid concentration of 5 mg/mL. The resulting liposomes exhibited both unilamellar and multivesicular morphology, falling within a size range of 180–1030 nm (SI Table S2). The liposomes were stored at 4 °C and used within a period of 2 to 3 weeks.

2.3 Electroformation

Electroformation was conducted at room temperature. For GUV formation on ITO-coated glass slides (50 × 60 mm, Präzisions Glas & Optik GmbH, Iserlohn, Germany), 36 µL of the liposome solution (5 mg/mL lipid or liposomes) was applied as droplets on the conductive side of each UV-cleaned glass slide and dehydrated for 30 min in a sealed chamber containing a saturated NaCl solution (Fig. 1a). The saturated NaCl solution was used to control the humidity during the dehydration step and to avoid complete dehydration of the sample, which would be critical in applications involving membrane proteins [36, 37]. Subsequently, a chamber was formed by separating the ITO-coated glass slides (conducting sides facing each other) with a 3-mm thick Teflon spacer containing copper tape. The chamber was sealed and filled with 1.5 mL GUV formation buffer. For the "non-ionic" GUV formation buffer (Table 1), an AC electric field (10 Hz, 0.4 –2.2 peak-to-peak voltage (V_{PP}), increasing every 6 min) was applied overnight.

For electroformation on platinum wires, 2 µL of the liposome solution (5 mg/mL lipid or liposomes) was deposited in 0.5-µL drops onto two parallel platinum wires (0.4 mm diameter, 8–9 mm length, 2–3 mm interelectrode separation) mounted in a custom-made Teflon chamber (Fig. 1b). The droplets were dried under vacuum (250 mbar) for 30 min in a sealed chamber containing a saturated NaCl solution. The chamber was filled with 340 µL GUV formation buffer. For "non-ionic" GUV formation with non-ionic buffer (Table 1), an AC electric field (10 Hz, 0.4–2.2 V_{PP}, increasing every 6 min) was applied overnight. For "ionic" GUV formation with ionic buffers (Table 1), an AC electric field (500 Hz, variable voltage 0.35 V_{PP}/1 V_{PP}/2 V_{PP}) was used overnight, based on previous studies showing that the use of ionic buffers demands higher frequencies [18, 19, 30, 38, 39]. After formation, GUVs were gently transferred into a 2-mL Eppendorf tube and stored at room temperature for 2 or 3 days.

2.4 Optical microscopy

To observe the giant vesicles under a microscope, 5 µL of electroformed vesicles was mixed with either 45 µL of non-ionic microscopy buffer or 45 µL of ionic microscopy buffer (Table 1) on a coverslip (26 × 76 mm, number 1.5, Thermo Scientific, Gerhard Menzel GmbH, Braunschweig, Germany). Microscopy and image acquisition were carried out using a Leica TCS SP5 II (Mannheim, Germany) or Leica TCS SP8 confocal laser scanning microscope (Leitz, Wetzlar, Germany) equipped with a white light laser and a 63 × water objective (1.2 NA). The following acquisition settings were applied: 2048 × 2048 logistical size, 400 Hz scan speed and a pinhole of 1 AU. A transmitted detection module with a photon-counting PMT was used to visualise the vesicles in a bright-field (BF)/differential interference contrast (DIC) mode (gain 400 V). A hybrid photodetector (HyD SMD 2) was used to detect the fluorescence emission in the range of 502–749 nm (excitation at 497 nm, gain 100 V, laser intensity 4.99%). Giant vesicles were observed under the microscope within 30 min, reducing the risk of unwanted vesicle collapse on the coverslip surface.

2.5 Image analysis

Image analysis was performed using the Fiji software in ImageJ (version 2.9.0/1.53t, Wayne, Rasband, S., U.S. National Institutes of Health, Bethesda, Maryland, USA. BF/DIC microscopy was used to focus on GVs and fluorescence microscopy to identify lamellarity. We categorised vesicles into three types: unilamellar (single lipid bilayer), multilamellar (onion-like concentric membranes), and multivesicular (multiple non-concentric inner vesicles). Vesicles were manually counted. The diameter of the GUVs was measured by drawing a line horizontally centred from one edge of the vesicle to the other. The outcomes were plotted using OriginPro 2023, and the statistical analysis was conducted using the same software.

3 Results and discussion

3.1 Giant vesicle generation from preformed liposomes: morphological diversity and electroforming efficiency

The classical technique for forming GUVs begins by dissolving lipids or lipid mixtures in an organic solvent, followed by depositing this solution as a thin lipid film on a supporting substrate. However, this approach has an inherent disadvantage in that there is a risk of denaturation of membrane proteins due to exposure to organic solvents. In this study, we aimed, therefore, to evaluate the electroforming of GUVs using preformed liposomes. To
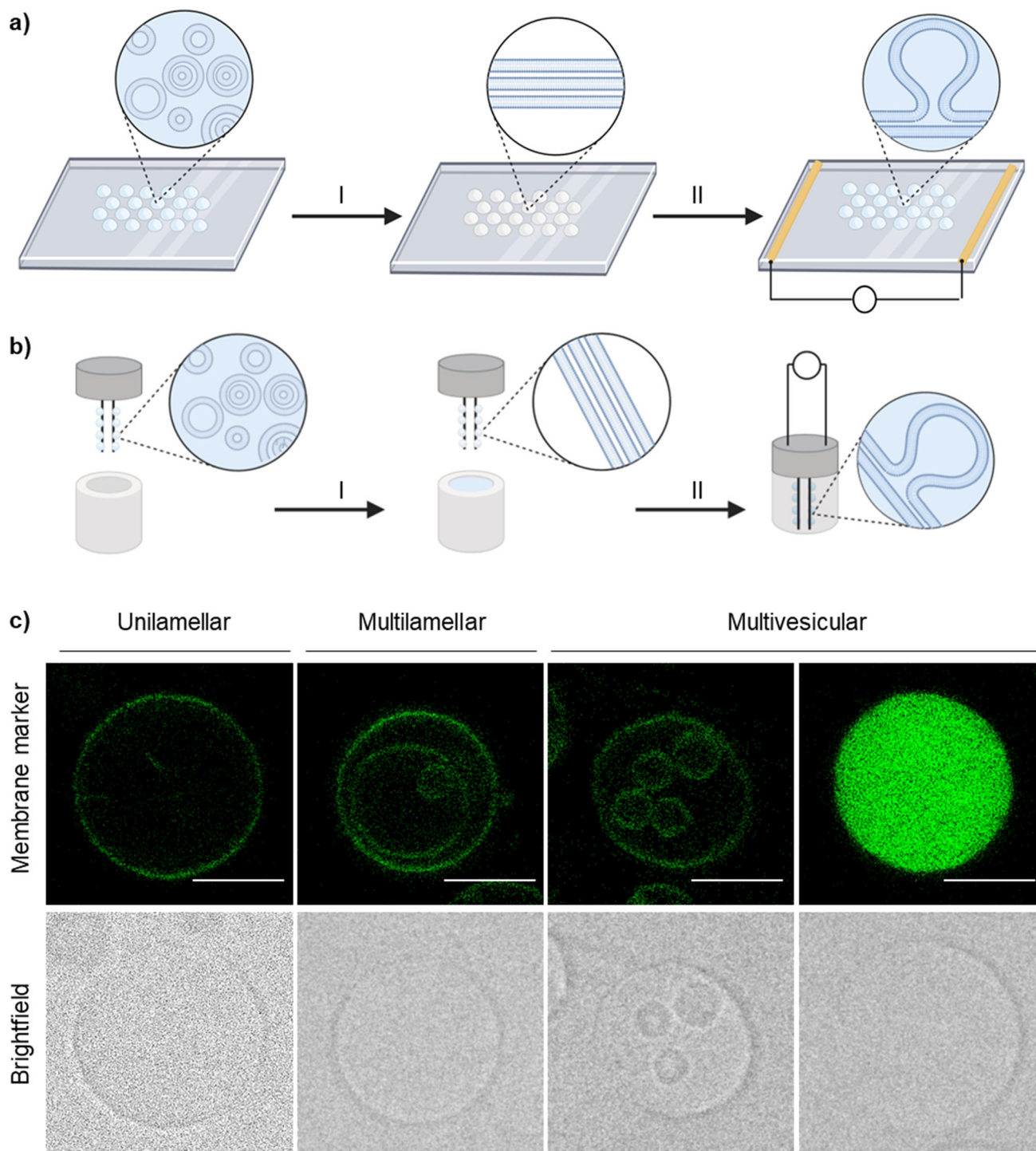
Fig. 1 Electroformation of giant vesicles and their morphology. Schematic representation of the GUV electroformation setups using ITO-coated glass slides (**a**) or platinum wires (**b**). Large liposomes applied on the indicated surfaces are partially dehydrated (step I). Subsequently, liposomes are rehydrated in GUV formation buffer in the presence of an AC electric field (step II), resulting in the formation of giant vesicles. Figures **a** and **b** were created with BioRender.com. **c** Exemplary confocal microscopy images of unilamellar (left), multilamellar (middle) and multivesicular (right) vesicles showing fluorescence signals corresponding to the membrane marker ATTO-DOPE (green) and bright-field channel (grey). Scale bars, 10 μm

study this process, we prepared large liposomes containing traces of a fluorescent marker lipid (ATTO488-DOPE, 0.1 or 0.2 mol%). These liposomes were then applied to either ITO-coated glass slides or platinum wires (Fig. 1; [14, 15, 18]). After partial dehydration in a desiccator, vesicles were rehydrated in the presence of an alternating electric field under non-ionic (300 mM sucrose) and ionic conditions (50 mM K_2SO_4). An ionic buffer containing K_2SO_4 was chosen because previous studies have demonstrated its ability to preserve the activity of reconstituted membrane proteins [40, 41]. For both conditions, the morphological analysis of generated giant vesicles (GVs) revealed three distinct types of GVs: unilamellar, multilamellar, and multivesicular, as illustrated by representative confocal images in Fig. 1c and reported in previous studies [26, 42–46]. In addition, a subset of vesicles termed "filled" GVs was observed that corresponded to tightly packed multivesicular vesicles, as demonstrated by a dithionite assay (SI Fig. S1). The prevalence of multivesicular vesicles in the preparations was related to the electroforming procedure using preformed vesicles, as this phenomenon was not observed to the same extent as when using direct lipid deposition from organic solvents (SI Fig. S2). Some GVs generated from preformed liposomes showed inward-pointing protrusions, such as tubes similar to the findings presented in [47]. However, these vesicles were not evaluated in this study. In general, the use of the platinum wire configuration consistently promoted more GV formation compared to the ITO-coated glass slide configuration, despite the larger surface area and higher total lipid content of the ITO-coated glass slides (SI Table S3). This result is consistent with a similar trend reported for GV electroformation from liposomes containing SNARE protein [33], while another group reported the opposite for the formation of GV using lipids from an organic solution [39].

3.2 Giant vesicle generation under non-ionic conditions

For all liposomes tested, electroforming on either ITO-coated glass slides or on platinum wires resulted in the formation of giant vesicles under non-ionic conditions, comprising predominantly GUVs and multivesicular vesicles (Fig. 2a, c). Notably, the use of ITO-coated glass slides for electroforming resulted in a larger population of multivesicular vesicles compared to the results obtained using platinum wires (cf. Fig. 2a, c). The increased prevalence of multivesicular vesicles in the preparations compared to direct lipid deposition from organic solvents (cf. Fig. 2 and SI Fig. S2) may be due to the presence of ions within the preformed liposomes. The presence of these ions has an effect on dehydration after deposition, and thus on the precise control of the GUV electroforming process [48]. In addition, their presence facilitates spontaneous swelling through osmotic pressure, further complicating the accurate control of GUV electroformation [49].

In both setups, electroformation from POPC liposomes resulted in a lower number of GUVs compared to DOPC liposomes. This result might be attributed to the higher main phase transition temperature (T_m) of POPC (T_m = − 2 °C) compared to DOPC (T_m = − 17 °C). The lower T_m of DOPC may facilitate easier separation and bending of the bilayer [20, 50–52]. Notably, the number of DOPG GUVs was comparable to that of DOPC GUVs, regardless of whether ITO-coated glass slides or platinum wires were used. In contrast, electroformation from liposomes containing DOPS or DOTAP produced only a limited number of giant vesicles with minimal presence of unilamellar vesicles, regardless of the surface used. This is consistent with data from lipid film electroforming, which reports the need for stronger electric fields to increase the yield of DOPS-containing GUVs [20, 43].

The production of GUVs containing positively charged DOTAP lipids has also proven challenging in the past [53, 54]. In a prior investigation, attempts to generate cationic GUVs from lipid films composed of DOPC:DOTAP (95:5, mol%) proved unsuccessful [53]. To overcome this limitation, the authors used a method that involves heat treatment of the ITO-coated glass slides at temperatures as high as 150 °C. This thermal annealing process facilitates the restoration of the ITO thin films, which can deteriorate over time due to ageing. However, despite the incorporation of the annealing process for the ITO glass slides, our attempts to enhance cationic GV formation from liposomes did not result in any noticeable improvement (data not shown). In order to address the potential problem of ageing of the ITO glass slides [53], an attempt was also made to generate DOTAP GUVs using new ITO glass slides for each sample, but this was not successful in our hands. Notably, Bian et al. chose 1-palmitoyl-2-oleoyl-sn-glycero-3-ethylphosphocholine as a positively charged lipid instead of DOTAP and achieved successful GUV formation at a maximum concentration of 15 mol% [54]. Furthermore, we observed that the formation of GV containing DOPE was favoured on ITO-coated glass slides, whereas DOPC and DOPG-containing vesicles showed superior formation on platinum wires. Taken together, these results indicate that the degree of lipid saturation, as well as the charge and size of the head group, influence the formation of giant vesicles from preformed liposomes in terms of number and morphology. The observed difference between the ITO and platinum wire setups is likely due to the variations in chamber geometry, chamber volume, and interelectrode spacing in combination with the applied electric field, which have been shown in previous studies to significantly influence the process of GUV formation [20, 33, 39]. For electroformation on platinum wires, the wire diameter may also be critical for the efficiency of GV formation [33].

The subsequent analysis focussed on the size distribution of the generated GUVs. On both ITO-coated glass slides and platinum wires, DOPG-containing liposomes generated smaller GUVs (between 1 and 15 μm), with respect to those formed from DOPC and DOPS lipids, consistent with observations from previous studies [20, 52].
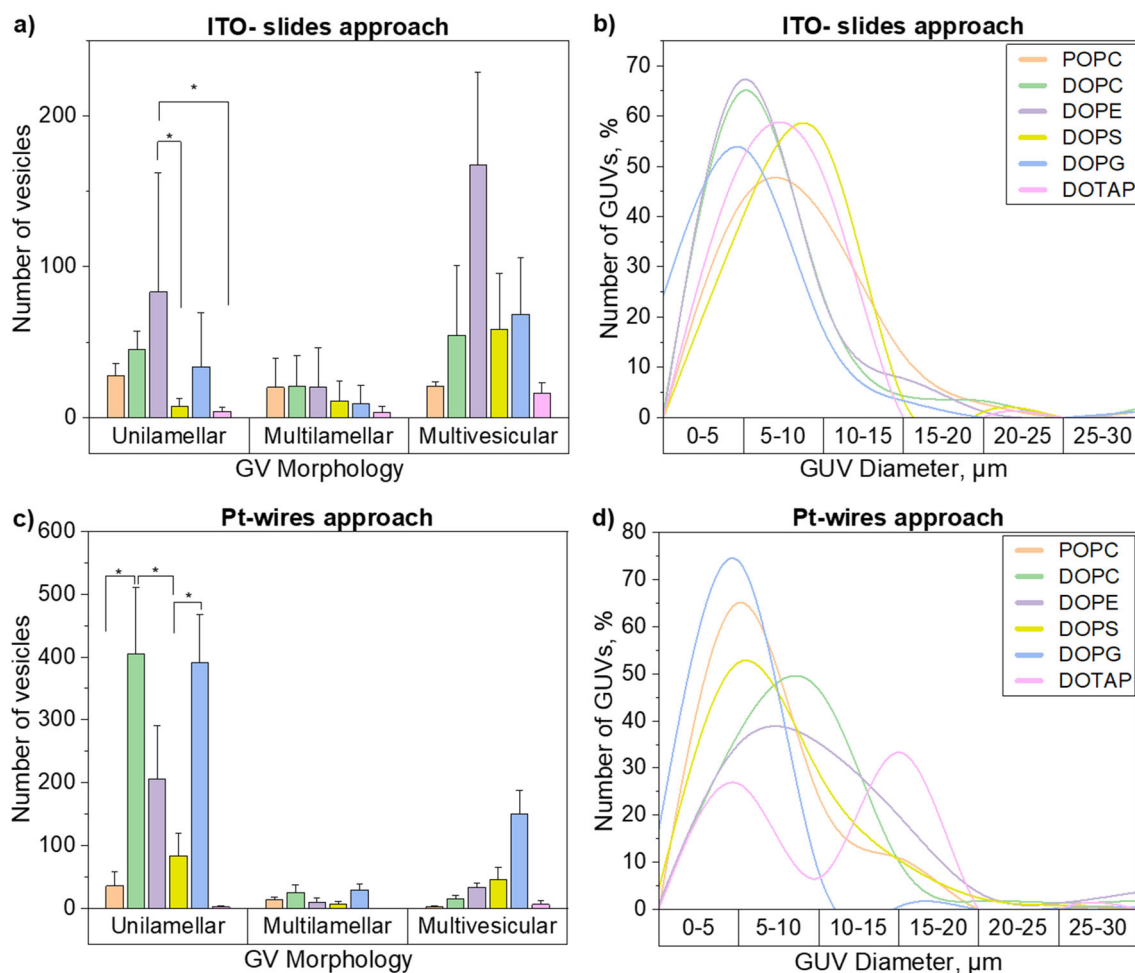
Fig. 2 Morphology and size distribution of giant vesicles formed from large liposomes under non-ionic conditions. Giant vesicles (GV) were formed from large liposomes composed of either POPC, pure DOPC or DOPC in a mixture with the indicated lipids (7:3 molar ratio). **a**, **c** Morphology distribution of the generated giant vesicles using ITO-coated glass slides (ITO-slides) or platinum wires (Pt-wires), as indicated. **b**, **d** Size distribution of giant unilamellar vesicles (GUV) generated using ITO-coated glass slides or platinum wires, as indicated. The number of vesicles and the diameter are calculated from the mean values of three independent experiments using 5 μL samples. Error bars correspond to the standard deviation. Asterisks indicate statistically significant differences (t-test, $P < 0.05$)

Notably, except for DOPG, GUVs generated on ITO-coated glass slides exhibited a slightly more constrained size distribution, ranging from 5 to 15 μm (Fig. 2b). In contrast, vesicles formed on platinum wires, which exhibited a broader size range of 5–20 μm (Fig. 2d). This phenomenon, previously reported in the context of electroformation from lipid films [33], was also observed during the formation of GUVs from DOPC films in the current study (see SI Fig. S2b) and is likely caused by the difference between the ITO and platinum wire setups, as discussed above.

3.3 Giant vesicle generation under ionic conditions

For electroformation under ionic conditions, we used an AC electric field with a frequency of 500 Hz, based on recommendations from previous studies [39]. We initiated our investigations by examining the effect of voltage on the abundance of giant vesicles. For this purpose, we performed experiments with different voltage settings (0.35, 1 or 2 V_{PP}), employing only the platinum wire setup with 2–3 mm interelectrode separation. As the voltage was increased, there was an observable rise in the number of giant vesicles, as depicted in Fig. 3a. This phenomenon was consistent across multiple groups, indicating a common trend in the formation of giant vesicles from lipids or liposomes [18–20, 55]. This trend was particularly pronounced in the case of GUVs derived from DOPG-containing liposomes. This observation is consistent with the findings of [18] and is in line with the electro-osmosis theory [14, 39, 46, 56]. A plausible explanation for the need for increased amplitude and frequency under ionic conditions lies in the significant accumulation of counterions near the electrode surface, leading to the development of an electric
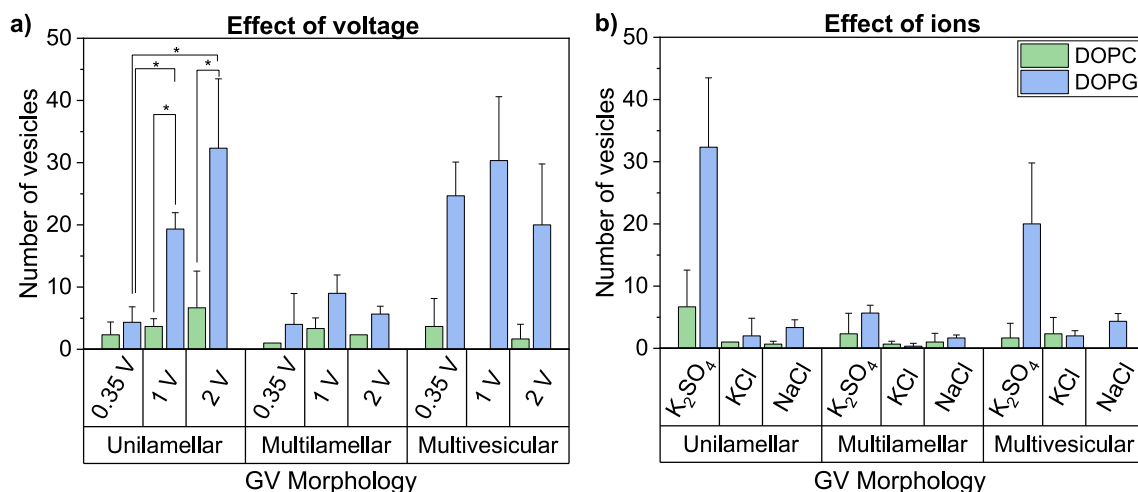
Fig. 3 Effect of voltage and ions on giant vesicle formation under ionic conditions using platinum wires. Giant vesicles (GV) were formed from large liposomes composed of either DOPC or DOPC:DOPG (7:3 molar ratio). **a** Effect of AC peak-to-peak voltage (V_{PP}) on giant vesicle yield (500 Hz, K_2SO_4 buffer). **b** Effect of ionic buffer composition on the giant vesicle yield (AC voltage of 2 V_{PP} and 500 Hz). The number of vesicles and the diameter are calculated from the mean value of three independent experiments using 15 μL samples. Error bars correspond to the standard deviation. The asterisk indicates statistically significant differences (*t*-test; $P < 0.05$)

double layer. Disruption of this electrical double layer could potentially manifest itself at higher frequencies [20]. In the case of GUVs containing anionic lipids (i.e. DOPG), the electrical repulsion between the charged lipids could facilitate the formation of giant vesicles by counteracting the intrinsic adhesive force between the membranes [42, 43]. The presence of ions increases the difference in conductivity between the lipid membrane and the electrolyte solution. This causes the solutions to diffuse across the lipid membrane, which then increases the negative surface tension from the electric field and further disrupts the lipid layer, promoting the formation of giant vesicles [14, 27].

In addition, this voltage adjustment induced a shift in the morphology distribution, favouring the formation of GUVs. In our study, we consciously abstained from escalating the amplitude beyond 2 V_{PP}. This precaution was taken to prevent lipid oxidation [57] and, consequently, to safeguard the integrity of the membrane protein during the formation of GUVs containing membrane proteins. In general, the number of GUVs was lower under ionic conditions compared to non-ionic conditions, as also shown in the previous study [19, 58].

We next investigated the effect of ions in the swelling buffer at a voltage of 2 V_{PP}. Interestingly, replacing K_2SO_4 with NaCl or KCl strongly reduced GUV formation, even in the presence of charged lipids (Fig. 3b). Similar to the group of Karmakar, could not form GUV in the presence of 100 mM NaCl [59]. In contrast, the group of von Ballmoos reported successful GUV formation both in the absence and presence of 100 mM NaCl or KCl [58]. For comparison, GUVs were generated in their study from a lipid mixture containing 70% DOPC and 30% DOPG in an organic solution. These findings underscore the notion that specific ions within the swelling buffer can wield a substantial influence on the efficacy of GUV formation when charged liposomes, rather than lipid films, are employed as the initial material for electroformation.

For all liposomes tested, GUVs were obtained at 2 V_{PP} under ionic conditions (K_2SO_4 buffer), with negatively charged liposomes (DOPG, DOPS) exhibiting a greater propensity to form GUVs (Fig. 4a). This suggests that the electrical repulsion between the charged lipids facilitates the formation of giant vesicles by counteracting the intrinsic adhesive force between the membranes [42]. The presence of ions increases the difference in conductivity between the lipid membrane and the electrolyte solution. This causes the solutions to diffuse across the lipid membrane, which then increases the negative surface tension from the electric field and further disrupts the lipid layer. This disruption promotes the formation of the giant vesicles [20, 42].

Furthermore, the GUVs formed under ionic conditions were generally larger in size, ranging from 5 to 25 μm, compared to those formed under non-ionic conditions (Figs. 2d, 4b). This phenomenon was also observed in GUV formation from lipid films, where the diameter of the GUVs increased with the NaCl concentration from 0 to 200 mM [20]. Overall, under ionic conditions, both the morphology and size of the GUVs exhibited greater heterogeneity under ionic conditions.
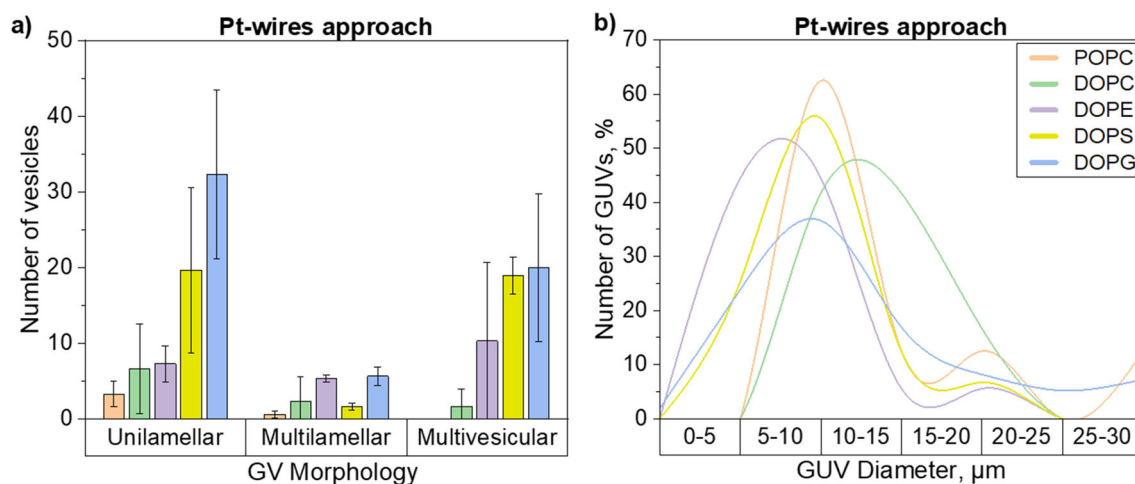
Fig. 4 Morphology and size distribution of giant vesicles (GV) formed from large liposomes under ionic conditions (K_2SO_4 buffer, AC voltage of 2 V_{PP}, 500 Hz) using platinum (Pt) wires. Giant vesicles were formed from large liposomes composed of either POPC, pure DOPC or DOPC in a mixture with the indicated lipids (7:3 molar ratio). **a** Morphology distribution of the generated GVs. **b** Size distribution of giant unilamellar vesicles (GUV). The number of vesicles and the diameter are calculated from the mean value of three independent experiments using 15 µL samples. Error bars correspond to the standard deviation. The asterisk indicates statistically significant differences (t-test; $P < 0.05$)

4 Conclusion and outlook

We have shown that electroformation of GUVs from preformed liposomes can be successfully achieved on both ITO-coated glass slides and platinum wires for a wide range of liposomal phospholipid compositions, but requires optimisation with respect to the buffer solution, ion type and electric field conditions. Electroformation on platinum wires in combination with the non-ionic condition generally gives a higher yield of GUVs, but even under ionic conditions, most experiments still produced GUVs, especially with liposomes containing negatively charged lipids. The liposomal approach offers a significant advantage over classical electroforming via lipid film deposition. It allows the direct use of liposomes containing membrane proteins, resulting in the generation of GUVs containing these proteins. Functional reconstitution via this approach under non-ionic conditions has been achieved for a number of membrane proteins without affecting their activity (SI Table S1). However, not all membrane proteins may retain their activity under these conditions. In this case, GUVs can be prepared in buffers containing higher salt concentrations by applying a voltage with a higher voltage and/or frequency ($\sim$ 2 V; $\sim$ 500 Hz; SI Table S1), but the yield of unilamellar vesicles is lower under these conditions. In this study, GUVs were prepared from liposomes of relatively simple lipid composition, but higher lipid complexity can be achieved by mixing liposome solutions of different compositions before electroformation [28, 60]. As membrane protein reconstitution is often challenging in complex lipid mixtures, especially those containing cholesterol, the use of this approach may pave the way for future investigations into the impact of complex lipid compositions on protein activity. By first efficiently reconstituting proteins into "simple liposomes" and later introducing the more complex lipid environment during GUV formation, this approach becomes a promising avenue for future research efforts. The versatility of the liposomal approach suggests its broad applicability without significant limitations. As a powerful tool, it promises to facilitate the study of membrane proteins in a cell-like model membrane system.

Author contributions

HDU, ZT and MC performed the GUV electroformation experiments. HDU and ZT analysed the data. HDU wrote the manuscript. RLL-M supervised the project at the University of Copenhagen. TGP supervised the project and revised the manuscript. All the authors reviewed and approved the final manuscript for submission.

Data availability The authors declare that the data supporting the findings of this study are available within the paper and its Supplementary Information files. Should any raw data files be needed in another format they are available from the corresponding author upon reasonable request.

Declarations

Conflict of interest The authors declare that no competing interests exist.

References

1. S.F. Fenz, K. Sengupta, Integr. Biol. Quant. Biosci. Nano Macro (2012). https://doi.org/10.1039/c2ib00188h
2. R. Dimova, Annu. Rev. Biophys. (2019). https://doi.org/10.1146/annurev-biophys-052118-115342
3. P.F.F. Almeida, A. Pokorny, A. Hinderliter, Biochem. Biophys. Acta. (2005). https://doi.org/10.1016/j.bbamem.2005.12.004
4. T. Baumgart, B.R. Capraro, C. Zhu, S.L. Das, Annu. Rev. Phys. Chem. (2011). https://doi.org/10.1146/annurev.physchem.012809.103450
5. R. Lipowsky, R. Dimova, J. Phys. Condens. Matter (2003). https://doi.org/10.1088/0953-8984/15/1/304
6. T. Bhatia, F. Cornelius, J.H. Ipsen, Biochem. Biophys. Acta. (2016). https://doi.org/10.1016/j.bbamem.2016.09.001
7. J. Kubiak, J. Brewer, S. Hansen, L.A. Bagatolli, Biophys. J. (2011). https://doi.org/10.1016/j.bpj.2011.01.012
8. J.F. Nagle, M.S. Jablin, S. Tristram-Nagle, Chem. Phys. Lipid. (2016). https://doi.org/10.1016/j.chemphyslip.2016.01.003
9. J.F. Baum, H.D. Uzun, T.G. Pomorski, Bio-Protoc. (2023). https://doi.org/10.21769/BioProtoc.4754
10. I.L. Jørgensen, G.C. Kemmer, T.G. Pomorski, Eur. Biophys. J. EBJ (2017). https://doi.org/10.1007/s00249-016-1155-9
11. H. Pick, A.C. Alves, H. Vogel, Chem. Rev. (2018). https://doi.org/10.1021/acs.chemrev.7b00777
12. O. Staufer, M. Schröter, I. Platzman, J.P. Spatz, Small. (2020). https://doi.org/10.1002/smll.201906424
13. F. Lussier, O. Staufer, I. Platzman, J.P. Spatz, Trends Biotechnol. (2021). https://doi.org/10.1016/j.tibtech.2020.08.002
14. M.I. Angelova, D.S. Dimitrov, Faraday Discuss. Chem. Soc. (1986). https://doi.org/10.1039/dc9868100303
15. D.S. Dimitrov, M. Angelova, Bioelectrochem. Bioenerg. (1988). https://doi.org/10.1016/0302-4598(88)80013-8
16. M. Angelova, D.S. Dimitrov, Progress in Colloid and Polymer Science. (1988). https://doi.org/10.1007/BFb0114171
17. C. Has, S. Pan, J. Liposome Res. (2021). https://doi.org/10.1080/08982104.2020.1730401
18. T. Pott, H. Bouvrais, P. Méléard, Chem. Phys. Lipid. (2008). https://doi.org/10.1016/j.chemphyslip.2008.03.008
19. H. Stein, S. Spindler, N. Bonakdar, C. Wang, V. Sandoghdar, Front. Physiol. (2017). https://doi.org/10.3389/fphys.2017.00063
20. Q. Li, X. Wang, S. Ma, Y. Zhang, X. Han, Colloids Surf. B Biointerfaces (2016). https://doi.org/10.1016/j.colsurfb.2016.08.018
21. S. Park, S. Majd, PLoS ONE (2018). https://doi.org/10.1371/journal.pone.0199279
22. M.K. Doeven, J.H.A. Folgering, V. Krasnikov, E.R. Geertsma, G. van den Bogaart, B. Poolman, Biophys. J. (2005). https://doi.org/10.1529/biophysj.104.053413
23. E.R. Geertsma, N.A.B. NikMahmood, G.K. Schuurman-Wolters, B. Poolman, Nat. Protoc. (2008). https://doi.org/10.1038/nprot.2007.519
24. L.C. Paweletz, S.L. Holtbrügge, M. Löb, D. de Vecchis, L.V. Schäfer, T.G. Pomorski, B.H. Justesen, Int. J. Mol. Sci. (2023). https://doi.org/10.3390/ijms241713106
25. A. Papadopulos, S. Vehring, I. López-Montero, L. Kutschenko, M. Stöckl, P.F. Devaux, M. Kozlov, T. Pomorski, A. Herrmann, J. Biol. Chem. (2007). https://doi.org/10.1074/jbc.M604740200

26. P. Girard, J. Pécréaux, G. Lenoir, P. Falson, J.-L. Rigaud, P. Bassereau, Biophys. J. (2004). https://doi.org/10.1529/biophysj.104.040360
27. H. Bouvrais, F. Cornelius, J.H. Ipsen, O.G. Mouritsen, Proc. Natl. Acad. Sci. U.S.A. (2012). https://doi.org/10.1073/pnas.1209909109
28. T. Bhatia, F. Cornelius, J. Brewer, L.A. Bagatolli, A.C. Simonsen, J.H. Ipsen, O.G. Mouritsen, Biochem. Biophys. Acta. (2016). https://doi.org/10.1016/j.bbamem.2016.03.015
29. J.-B. Manneville, P. Bassereau, D. Lévy, J. Prost, Phys. Rev. Lett. (1999). https://doi.org/10.1103/PhysRevLett.82.4356
30. S. Aimon, J. Manzi, D. Schmidt, J.A. Poveda Larrosa, P. Bassereau, G.E.S. Toombes, PLoS ONE (2011). https://doi.org/10.1371/journal.pone.0025529
31. V. Betaneli, E.P. Petrov, P. Schwille, Biophys. J. (2012). https://doi.org/10.1016/j.bpj.2011.12.049
32. P. Streicher, P. Nassoy, M. Bärmann, A. Dif, V. Marchi-Artzner, F. Brochard-Wyart, J. Spatz, P. Bassereau, Biochimica et Biophysica Acta (BBA) Biomembr. (2009). https://doi.org/10.1016/j.bbamem.2009.07.025
33. A. Witkowska, L. Jablonski, R. Jahn, Sci. Rep. (2018). https://doi.org/10.1038/s41598-018-27456-4
34. K. Bacia, C.G. Schuette, N. Kahya, R. Jahn, P. Schwille, J. Biol. Chem. (2004). https://doi.org/10.1074/jbc.M407020200
35. A. Berthaud, F. Quemeneur, M. Deforet, P. Bassereau, F. Brochard-Wyart, S. Mangenot, Soft Matter (2016). https://doi.org/10.1039/c5sm01654a
36. P.W. Winston, D.H. Bates, Ecology **41**, 232 (1960). https://doi.org/10.2307/1931961
37. A. Varnier, F. Kermarrec, I. Blesneac, C. Moreau, L. Liguori, J.L. Lenormand, N. Picollet-D'hahan, J. Membr. Biol. (2010). https://doi.org/10.1007/s00232-010-9227-8
38. M. Garten, S. Aimon, P. Bassereau, G.E.S. Toombes, J. Vis. Exp. JoVE (2015). https://doi.org/10.3791/52281
39. P. Lefrançois, B. Goudeau, S. Arbault, Integr. Biol. Quant. Biosci. Nano Macro (2018). https://doi.org/10.1039/c8ib00074c
40. S. Veshaguri, S.M. Christensen, G.C. Kemmer, G. Ghale, M.P. Møller, C. Lohr, A.L. Christensen, B.H. Justesen, I.L. Jørgensen, J. Schiller, N.S. Hatzakis, M. Grabe, T.G. Pomorski, D. Stamou, Science (2016). https://doi.org/10.1126/science.aad6429
41. R.M. Kühnel, M. Grifell-Junyent, I.L. Jørgensen, G.C. Kemmer, J. Schiller, M. Palmgren, B.H. Justesen, T. Günther Pomorski, Analyst (2019). https://doi.org/10.1039/C8AN02161A
42. K. Akashi, H. Miyata, H. Itoh, K. Kinosita, Biophys. J. (1996). https://doi.org/10.1016/S0006-3495(96)79517-6
43. N. Rodriguez, F. Pincet, S. Cribier, Colloids Surf. B Biointerfaces (2005). https://doi.org/10.1016/j.colsurfb.2005.01.010
44. W. Li, Q. Wang, Z. Yang, W. Wang, Y. Cao, N. Hu, H. Luo, Y. Liao, J. Yang, Colloids Surf. B Biointerfaces (2016). https://doi.org/10.1016/j.colsurfb.2015.11.020
45. E. Rideau, R. Dimova, P. Schwille, F.R. Wurm, K. Landfester, Chem. Soc. Rev. (2018). https://doi.org/10.1039/C8CS00162F
46. T.J. Politano, V.E. Froude, B. Jing, Y. Zhu, Colloids Surf. B Biointerfaces (2010). https://doi.org/10.1016/j.colsurfb.2010.03.032
47. J. Steinkühler, P. de Tillieux, R.L. Knorr, R. Lipowsky, R. Dimova, Sci. Rep. (2018). https://doi.org/10.1038/s41598-018-30286-z
48. P. Walde, K. Cosentino, H. Engel, P. Stano, Chembiochem Eur. J. Chem. Biol. (2010). https://doi.org/10.1002/cbic.201000010
49. P. Méléard, L.A. Bagatolli, T. Pott, Methods Enzymol. (2009). https://doi.org/10.1016/S0076-6879(09)65009-6
50. T. Shimanouchi, H. Umakoshi, R. Kuboi, Langmuir (2009). https://doi.org/10.1021/la8040488
51. H. Bi, B. Yang, L. Wang, W. Cao, X. Han, J. Mater. Chem. A (2013). https://doi.org/10.1039/c3ta10323d
52. S.E. Ghellab, W. Mu, Q. Li, X. Han, Biophys. Chem. (2019). https://doi.org/10.1016/j.bpc.2019.106217
53. C. Herold, G. Chwastek, P. Schwille, E.P. Petrov, Langmuir ACS J. Surf. Colloids (2012). https://doi.org/10.1021/la3005807
54. T. Bian, J.M. Autry, D. Casemore, J. Li, D.D. Thomas, G. He, C. Xing, Biochem. Biophys. Res. Commun. (2016). https://doi.org/10.1016/j.bbrc.2016.10.096
55. P.K. Hanson, L. Malone, J.L. Birchmore, J.W. Nichols, J. Biol. Chem. (2003). https://doi.org/10.1074/jbc.M305263200
56. D.S. Dimitrov, M.I. Angelova, Prog. Colloid Polym. Sci. (1987). https://doi.org/10.1007/3-798-50724-4_62
57. Y. Zhou, C.K. Berry, P.A. Storer, R.M. Raphael, Biomaterials (2007). https://doi.org/10.1016/j.biomaterials.2006.10.016
58. N. Dolder, P. Müller, C. von Ballmoos, Soft Matter (2022). https://doi.org/10.1039/d2sm00551d
59. A. Basu, P. Maity, P. Karmakar, S. Karmakar, J. Surf. Sci. Technol. (2016). https://doi.org/10.18311/jsst/2016/7753
60. C.C. Vequi-Suplicy, K.A. Riske, R.L. Knorr, R. Dimova, Biochem. Biophys. Acta. (2010). https://doi.org/10.1016/j.bbamem.2009.12.023